

## REVIEW

## Some physical aspects of positron annihilation tomography: A critical review

B. N. Ganguly,<sup>1\*</sup> N. N. Mondal,<sup>1</sup> M. Nandy,<sup>1</sup> F. Roesch<sup>2</sup>

<sup>1</sup> Saha Institute of Nuclear Physics, Kolkata-700064, India

<sup>2</sup> Institute of Nuclear Chemistry, University of Mainz, Mainz, D-55128, Germany

(Received March 10, 2008)

Positron emission tomography (PET) is an imaging modality for medical diagnoses that can determine biochemical and physiological processes in vivo in a quantitative way by using radio-pharmaceuticals labeled with positron emitting radionuclides. This article brings together various aspects of the basic physics, critical design and instrumentation along with the modalities of the application of radiotracers and the radiological protections involved in the processes. A critical discussion on the various aspects of the PET system is also included. Several new advances and scope of future investigations in terms of better sensitivity, local as well as kinetic resolution, specific tracer targeting (including chemical speciation) and better spatial resolution of the PET image are also covered.

### Introduction

Positron emission tomography (PET) is a state of the art molecular imaging technology used in medical diagnoses and biomedical research to identify images of radio-labeled probes at molecular level, that reveal the physiological and biochemical functions of the different parts of the organs in vivo.<sup>1</sup> The main emphasis lies on the functional imaging of the tissues as compared to classical X-ray images, computerized tomography (CT-CAT) or magnetic resonance imaging (MRI), which probe the static structure and morphological properties of the tissues.<sup>2</sup> The first attempt<sup>3</sup> of a PET system was made as early as in 1960s. Later only in 1975, the first industrial PET scanners had arrived, since there had been extremely time consuming and lengthy reconstruction algorithms and special radiochemical tracer requirements. Thereafter, vast improvements both in electronics and detector systems as well as the nuclear medicine aspects have changed the scenario and PET now emerges as the latest molecular imaging technology that cuts through the darkness non-invasively, probing the minute details of the molecular changes happening in vivo.

PET imaging actually depends on the distribution and adsorption/localization of positron emitting radiotracers incorporated within the body, in the form of radio-pharmaceuticals. Hence, PET images depict the concentration distribution (quantitative) of the radio-tracer in the form of chemical compounds (tracer kinetic method) within a particular section or the whole body. Thus, it is emphatically the physiological picture concerned that actually complements the anatomical information and is useful for diagnosis at a very early stage (almost at the onset of the diseases) of cancer,

heart malfunctioning and disorders of the brain or of neuro-genic origin, such as: epilepsy, stroke and dementia. Apart this, it also serves as a basic research tool to study the functional anatomy, especially of such delicate organs like brain. Today, the technique is also being utilized by the pharmaceutical industries to test the application of new drugs before its actual implementation.<sup>4</sup> In this article, we shall discuss the physico-chemical basis of PET and various scopes of improvements, highlighting the need of further experimentation for the benefit to be accrued towards the finesse in medical diagnoses.

### Physics and instrumentation of PET

The basic idea of the technique originates from the chemical binding of the positron emitting radioisotope (e.g., <sup>18</sup>F, and <sup>11</sup>C and also other positron emitter metallic radionuclide like <sup>68</sup>Ga) to a particular targeting vector. These radioisotopes emit positrons which subsequently annihilate emitting two photons, back to back (nearly 180°) with  $E_\gamma = 511$  keV, corresponding to the rest mass of electron and positron.

The maximum kinetic energy of a positron after its emission is typically within 1 MeV (from most commonly used radioisotopes like <sup>18</sup>F or <sup>11</sup>C) for which the calculated range of ~0.5 mm to 2 mm in the human tissue is possible (the maximum range can be calculated through a range energy relation<sup>5</sup> assuming a density approximately like water) before the annihilation takes place. A schematic representation of the same is given in Fig. 1. These photons are detected in coincidence in a detector array (a ring system) around the section of specimen under consideration for the assay of the origin

\* E-mail: bichitra.ganguly@saha.ac.in

of source (Fig. 2). Thus in a PET tomograph, the detectors are electronically coupled to several pairs, as if, each pair is observing a line of response to measure an event within a fixed time window. Further, image reconstruction and position resolution are some of the important crucial factors which are indeed limited by several physical effects, which shall be dealt with subsequently.

*Source of positron*

The first step of a PET examination is the injection of a radioactive tracer, i.e., the positron ( $\beta^+$ ) emitter in the body of the specimen (animal or patient). All positron emitting nuclei are proton rich (neutron deficient in comparison to its nearest stable isobars). Positron emission from the nucleus is secondary to the conversion of a proton into a neutron as in:  $p \rightarrow n + \beta^+ + \nu$ , where a positron and neutrino are emitted. Positron is the antiparticle (antimatter conjugate) of electron, emitted in  $\beta^+$  decay. Positron has an initial kinetic

energy after its emission and can take up a continuum of values up to a maximum. For a simple illustration, a table (Table 1) of short-lived isotopes commonly used in PET, a representation of the decay scheme and the energy spectrum of  $\beta^+$  emission from  $^{68}\text{Ga}$  (although it is not very common but very specific, chosen as an example) is given (Fig. 3).

Positrons take an extremely tortuous passage through the matter losing its kinetic energy in ionizing events or in inelastic scattering or in producing excited molecular species and free radicals and eventually thermalize within  $10^{-11}$  seconds. Diffusion after thermalization until annihilation involves distances of only about hundreds of nanometers, the de Broglie wavelength of a positron at room temperature is  $\sim 7.5$  nm. Positron lifetimes in molecular media are nearly  $\sim 400\text{--}500$  ps after which they may annihilate as free positrons.<sup>6</sup> However, a fraction of positrons may form positronium (Ps), in molecular substance and its fraction varies from medium to medium.

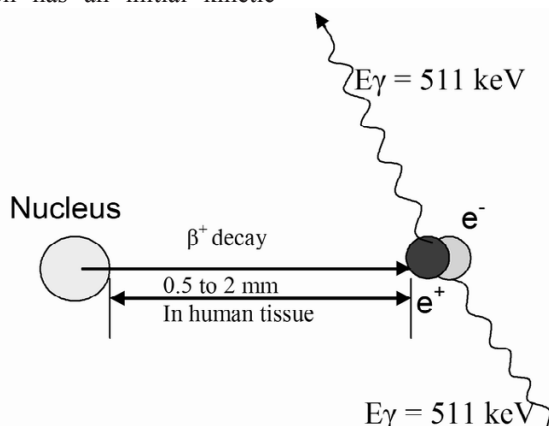


Fig. 1.  $e^+e^-$  annihilation in biological medium

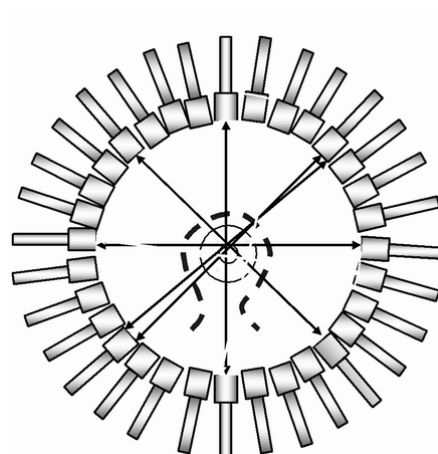


Fig. 2. Array of PET detectors: circularly arranged in a single ring (two-dimensional figure). The arrows are showing the true lines of response

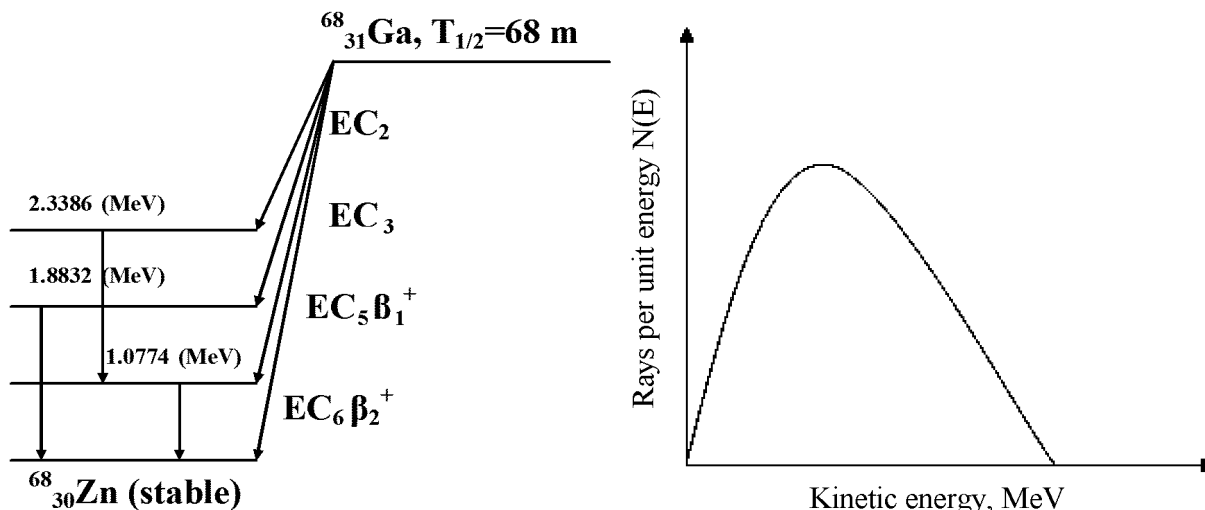


Fig. 3. Decay scheme of <sup>68</sup>Ga source and energy distribution of positrons (HABER et al., 1990)

Table 1. Some radioisotopes used in PET

Radionucleus	Half-life, min	E(e <sup>+</sup> ) <sub>max</sub> , MeV	Nuclear reaction	Comment
<sup>11</sup> C	20.334	0.960, mean 0.385	<sup>14</sup> N(p, α) <sup>11</sup> C	No γ, 99.75% e <sup>+</sup>
<sup>13</sup> N	9.965	1.19, mean 0.491	<sup>16</sup> O(p, α) <sup>13</sup> N	No γ, 99.8 % e <sup>+</sup>
<sup>15</sup> O	2.03	1.73, mean 0.735	<sup>14</sup> N(d,n) <sup>15</sup> O	No γ, 99.9% e <sup>+</sup>
<sup>18</sup> F	109.7	0.633, mean 0.249	<sup>18</sup> O(p,n) <sup>18</sup> F	No γ, 96.73% e <sup>+</sup>
<sup>68</sup> Ga	67.71	1.898, mean 0.74	<sup>68</sup> Ge → generator produced <sup>68</sup> Ga	4 γ, 89.14% e <sup>+</sup>

For the Ps formation, its application in liquids and molecular substances, the proponents of the spur model<sup>7</sup> or diffusion recombination model,<sup>8</sup> showed that positron deposits its energy in discrete quantities, nominally about a hundred electron volts, which produces ripples of excited and ionized molecules. Each spur on the track is thus a microcosm containing a set of reactive species. These evolve temporally and spatially by diffusing and by reacting with each other and with any solutes present. Positronium is formed when the positron succeeds in finding a quasi-free electron before the later may indulge in the geminate recombination effect. Formation of Ps (ortho and para positronium in the ratio of 3:1) is thus an important consequence in the molecular medium, which is signaled by the characteristic pick-off lifetime of the ortho positronium component and observations of the para positronium (singlet) narrow component in the angular correlation of annihilation radiation (ACAR) spectra. So far, the contribution and reaction of Ps in biological medium, for the PET research has been completely ignored.

### Annihilation radiation

As the electrons and positrons are anti-particle of each other, there is a finite probability that these two particles will interact, annihilate and produce photons. Positron annihilation event is governed by quantum electrodynamics (see the FEYNMAN<sup>9</sup> diagrams, Fig. 4.) The dominating influences are: nature's apparent reluctance to create photons: as each extra photon costs a factor of a  $\alpha = 1/137$ , the fine structure constant (which is a fundamental physical constant, characterizing the strength of the electromagnetic interaction) a reduction in free space, its reluctance to transfer momentum between dissimilar mass and the requirement of spin conversion. In principle, any number of photons may be produced in any annihilation event within the constraints of conservation laws. While one photon annihilation requires a third body, a two photon annihilation requires none. Since all the conservation laws are satisfied by the two photons themselves, this interaction is by far the most common. The conserved quantities are: (1) energy (=1.02 MeV if the electron and positron are at rest or possess low momentum), (2) linear momentum, and (3) spin (S=0 or 1).

Radiation detectors

Interaction of ionizing radiation with the detector is measured in terms of the total energy deposited by radiation up on passage through the detector. Typically this energy is converted into a measurable electrical signal or charge. The ability of the radiation detector to accurately measure the deposited energy (for example in PET, the incident radiation energy is 511 keV), is of paramount importance. Generally, inorganic scintillation detectors are used for these purposes which have very high efficiency light output. The accuracy of measurement is characterized by the width of the

photopeak in the energy spectrum, and is referred to as the energy resolution (a dimensionless number and is defined as the ratio of the full width at half maximum, FWHM, of the photopeak to its centroid position) of the detector. One may consult these aspects from Reference 10. As mentioned, scintillators are by far the most common and successful mode for detection of 511 keV photons in PET imaging due to their good stopping efficiency and energy resolution. These are coupled to photodetector devices for the detection of the electrical signal. A classification of the scintillators together with their characteristic properties is given in Table 2.

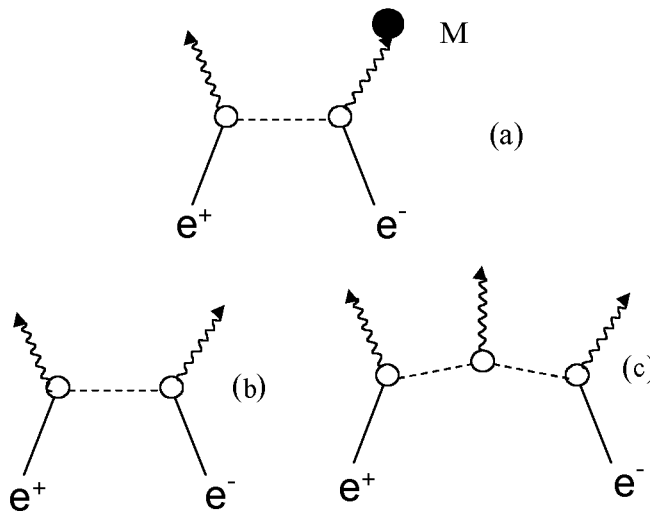


Fig. 4. Feynman diagrams for (a) one photon, (b) two photon and (c) three-photon positron annihilations. Filled in vertex is equivalent to the third power of the fine structure constant, signifying the unfavorable momentum transfer to a heavy object. The open vertices correspond to photon creation, equivalent to the first power of the fine structure constant (FEYNMAN, 1982)

Table 2. Different types of inorganic scintillators used for radiation detection in PET and their properties concerning the light output (as compiled from different sources)\*

Scintillator	Light yield, photons/keV	Relative light output, %	Decay time, ns	Density, g/cm <sup>3</sup>	Hygroscopic	Refractive index	Comment
NaI(Tl)	38	100 (λ <sub>nm</sub> = 410)	250	3.67	yes	1.85	Excellent energy and good time resolutions
BGO	10	20 (λ <sub>nm</sub> = 480)	300	7.13	no	2.15	Compact detector, low after glow
LYSO	26	68 (λ <sub>nm</sub> = 430)	53	7.4	no	1.81	Good light output, used in phoswich detectors
BaF <sub>2</sub>	1.8	5 (λ <sub>nm</sub> = 220)	0.6–0.8	4.88	slightly	1.54	Fast component for fast time resolution
LSO	32	75 (λ <sub>nm</sub> = 420)	41	7.1	no	1.81	Excellent time resolution
YAP(Ce)	18	40 (λ <sub>nm</sub> = 420)	27	5.55	no	1.94	Light output is stable with temperature
GSO	10	25 (λ <sub>nm</sub> = 440)	60	6.71	no	1.91	Uniform light output
LaBr <sub>3</sub> (Ce)	63	130 (λ <sub>nm</sub> = 380)	26	5.29	yes	1.9	Higher light output than NaI(Tl), timing properties quite good, resolution is better

\* [http://www.mt-berlin.com/frames\\_cryst/descriptions/scintillators\\_gen](http://www.mt-berlin.com/frames_cryst/descriptions/scintillators_gen), Reference 11, and <http://www.detectors.saint-gobain.com>, [http://www.sinocera.net/en/crystal\\_lyso.asp](http://www.sinocera.net/en/crystal_lyso.asp)

In the latest development, it is found that gadolinium oxy-orthosilicate doped with cerium (GSO) constitutes to be a useful PET detector because of its better energy resolution and more uniform light output despite its low stopping power and light output. Finally, the extremely short decay time of BaF<sub>2</sub> (600 ps for the emitted photons in UV region) is an ideal crystal for use in time-of-flight (TOF) scanners which helps to compensate partially for the low sensitivity arising due to the reduced stopping power of these scintillators. The most recently employed crystals reported (Table 2) are however, Ce doped lanthanum bromide (BrilLanCe-380), is a good candidate for PET with excellent light output. Its timing properties are suitable for TOF-PET measurements. Newer crystals like CeBr<sub>3</sub> also offer better possibilities (<http://www.nss-mic.org/2006/Program/ListProgram.asp?session=N43>) for TOF-PET, which require a high light output as well as good timing resolution. At present using these crystals a time resolution of about 166–170 ps has been reached with Hamamatsu R4998 fast photomultipliers.

Photo-detectors used in scintillation detection for PET are in two categories, namely the photomultiplier tubes (PMTs) and the semiconductor based photodiodes. PMTs are the most reliable devices to measure and detect low levels of scintillation light. An incoming scintillation photon deposits its energy at the photocathode and triggers the release of a photoelectron. This consequently opens up the sequence of electron multiplication and acceleration through several stages of dynodes, within a PMT. It is important to note: the high gain obtained from such a device yields very good signal to noise ratio for low light levels and is the primary reason for its applicability in scintillation detection.

Recently, there have been finer structural developments, in PMTs to maximize the gain and reduce the travel time of the electrons from cathode to anode, as well as reduce the variation of travel times of individual electrons. For example a fine grid dynode structure has been developed which restricts the spread of photoelectrons while in trajectory, thereby making a position-sensitive energy measurement within a single photomultiplier tube (PS-PMT). Also, more recently a 2D array of glass capillary dynodes (each of which is few microns wide) have been introduced, and multi mode structure is used for electron collection, thereby providing a dramatically improved position sensitive energy measurement (multi channel PMT, MC-PMT).

Photodiodes on the other hand are based upon semiconductors, which have high sensitivity for detecting significantly lower energy photons. These detectors typically are in the form of PIN diodes (PIN refers to the three zones of the diode: P-type, Intrinsic, N-type). The incident scintillation photons produce electron-hole pairs in the detector and an applied electric field then results in a flow of charge that can be

measured through an external circuit. But due to the presence of thermally activated charge flow and very low signal amplification, it suffers from the disadvantage of poor signal to noise ratio. With the recent use of Avalanche Photo Diode (APD), where an internal amplification of the signal is provided, the signal is, however, better sensed,<sup>12</sup> but the APD gains become sensitive to small temperature variations as well as changes in applied voltage.

Finally, the scintillation crystals need to be coupled to photo-detectors for signal read out in a PET detector. There can be one to one coupling, where a single crystal is glued to an individual photo-detector; a close-packed array of small discrete detectors can then be used as a large detector that is needed for PET imaging. In order to improve the spatial resolution, in one to one coupling, very small size photo-detectors are needed, which calls for the need of APDs although there are practical difficulties as stated above. The other option is the coupling of individual channels of a PS-PMT or MC-PMT to the small crystals. Due to large package size of these photomultiplier tubes, tactical alignment is needed to get a closed packed arrangement of the crystals in the scanner design.<sup>13</sup>

There are other important but fundamental aspects of sensing the signals from the detector assembly, namely the timing resolution and coincidence detection. Since in PET detector, the detection of two photons originating from a single coincident event is involved, that may originate from anywhere within the scanner field-of-view (FOV). Thus and by the distance traveled by each of them before interaction in the detectors, it will be different. For a typical whole body scanner, this distance can be as large as the scanner diameter (about 100 cm), the maximum time difference in the arrival of individual photons is of the order of about 3–4 ns (serves as a crude estimate for maximum range, as guided by the fact that photon travel 1 m in 3.3 ns). Thus, the coincidence timing window even in the case of very fast scintillators like BaF<sub>2</sub> (where the timing resolution may be small), cannot be less than 3–4 ns because of the difference in the arrival times of the two photons emitted at the edge of the scanner field of view, as this would impose restriction in the transverse field of view.

However, the occurrence of random coincidences are a direct consequence of having a large coincidence timing window, they decrease the signal to noise ratio and decrease the PET image contrast if no correction factor is applied.<sup>14</sup> So, there has to be an optimization of the chosen coincidence window, detector resolution and the decay rate of the pulses from the detectors. A good detector energy resolution (which is a function of the relative light output of the scintillator and its intrinsic energy resolution) allows very narrow energy gate and thus a more extensive and accurate rejection of scatter coincidences through an energy gating technique.

Finally, the sensitivity of the PET scanner is due to its ability to detect the coincident photons emitted from inside the scanner field of view, and it depends upon the scanner design, its geometry and the stopping efficiency of the detectors for 511 keV photons. The stopping power of the detector is dependent on its density and  $Z_{eff}$  of the crystal used. Thus, nowadays Ce doped lanthanum orthosilicate crystals (with Lu or Y) are gaining importance, as discussed above. Since sensitivity depends on the mean attenuation length of the crystals for 511 keV gamma-photons, proper choice of the detector size (thickness) would help to reduce the parallax error due to the photons which subtend oblique angle (typically annihilation photons at large radial distance from the central detector axis), as the measured position of energy deposition may carry large deviation. Thus, an on going research interest focuses in depth on interaction measurement and use of phoswich detectors<sup>15</sup> (CARRIER et al., 1988), where thin layers of different scintillators are stacked on top of each other (Fig. 5). The depth of interaction is identified through examination of the different signal decay times for the scintillators, via pulse shape discrimination technique. Good optical coupling is of course necessary with the photo-detectors to attain good spatial as well as energy resolution.

*PET instrumentation*

This is an area that has continued to evolve rapidly with an emphasis on increased sensitivity, improving

resolution and decreasing patient scanning times. Event detection in PET relies on electronic collimation, i.e., basically the line of response. An event is taken to be valid when (1) two photons are detected within a predefined electronic time window known as the coincidence window, (2) the subsequent line-of-response formed between them is within a valid acceptance angle of the tomograph and (3) the energy deposited in the crystal by both photons is within the selected energy window. Apart from these, there can be multiple events, scatter and random events which need to be filtered employing suitable methods before proceeding for the image reconstruction processes. Further, the sensitivity of a tomograph is determined by a combination of the radius of the detector ring, the axial length of the active volume for acquisition, the total axial length of the tomograph, the stopping power of the scintillators detector elements, packing fraction of the detectors and the other operative settings such as energy window, etc.

As PET uses coincidence detection, the detectors have to encompass 360° for complete sampling. The geometry and the co-ordinate system that is conventionally used is shown in Fig. 6.<sup>16</sup> The individual detector elements form coincidence pairs with opposing detectors (both in plane and axially) are mapped to a sinogram space, i.e., projections  $p(s, \phi, \theta, z)$  to further collect the PET data which is used to reconstruct images in tomography. This is illustrated in Fig. 7.

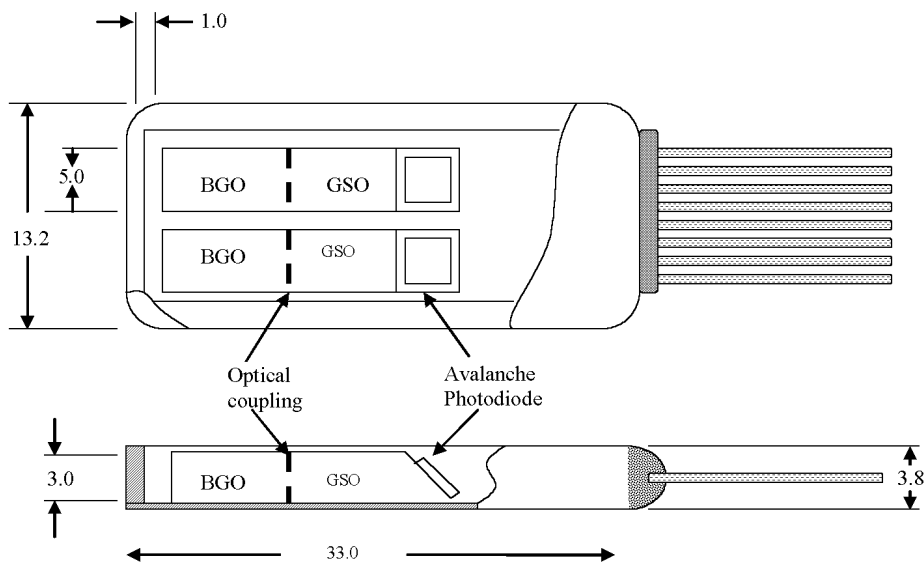


Fig. 5. Schematic representation of the dual channel quad scintillator detector module, one avalanche photodiode per two crystals have been used. Here, scintillators with different decay times, e.g., BGO ( $\tau = 300$  ns) and GSO ( $\tau = 60$  ns) are coupled and independent processing of the two detector channels through pulse-shape discrimination of the photodiode signals, the crystal of interaction is correctly identified. The dimensions shown are in mm

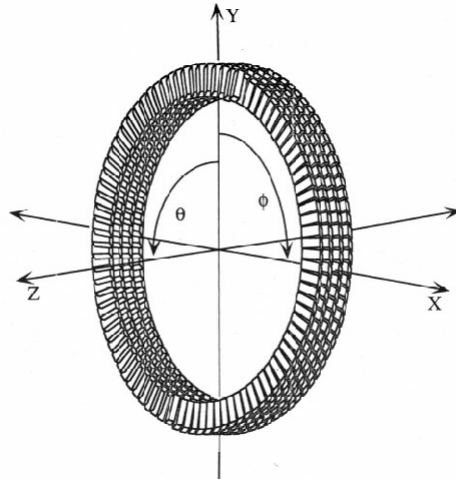


Fig. 6. Diagram of a full ring camera is shown with the coordinate system that describes the orientation of the camera. The azimuthal angle (rotated X-Y plane around the object,  $\phi$ ) is measured around the ring, while the polar angle (the angle the X-Y plane makes with Z axis,  $\theta$ ) is the measure of the angle between the rings, that is specially needed for 3D PET

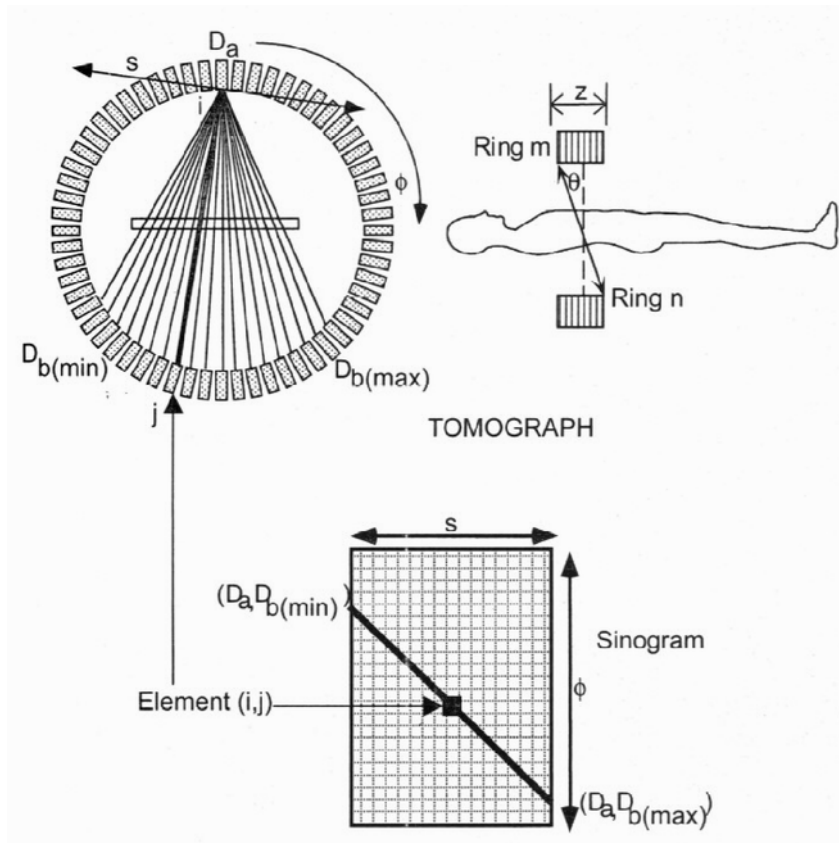


Fig. 7. Mapping from sampling projections to sinograms is shown. The transaxial field of view of a PET tomograph is defined by the acceptance angle in the plane. The electronics permits an individual detector to be in coincidence with a finite number of detectors in the opposing side of the ring forming a "fan". The fan angle of acceptance in the ring in the top left corner maps to a diagonal line in the sinogram

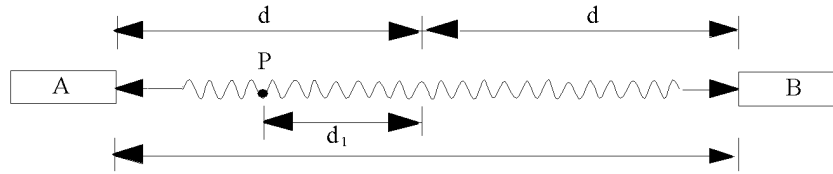


Fig. 8. Time-of-flight measurement; P marks the annihilation point from where the two photons originate and are recorded in detectors A and B

### Time-of-flight measurement in PET (TOF-PET)

Besides reducing the number of random coincidences, the input as timing information of the arrival of photons to the detectors can be used as a parameter to locate the points of annihilation and thus improve in the image reconstruction procedure. Figure 8. illustrates the afore said discussion, to identify the position of annihilation event. If it is assumed that P is the point position of annihilation event, it is thus observed from the figure that a photon moving along PA will travel a distance  $d-d_1$  while the other coincident photon will travel a total distance  $d+d_1$ . The difference of the distance traveled by one of the photons  $=2d_1$ , relative to the other. This can be calculated from  $2d_1=c \delta t$  where  $c$  is the speed of light (photons,  $c=3 \cdot 10^8 \text{ m}\cdot\text{s}^{-1}$ ), the coincident detectors measures the time difference in arrival times ( $\delta t$ ) of the two photons. It is realized that the time difference increases if the annihilation site is farther away from the midway between the two detectors. For simplicity, though here it is illustrated with only two detectors, the actual situation is not very simple. But if this timing input can be properly manipulated, and used to constrain the reconstruction algorithm (since it is expected to localize the annihilation site to within a few centimeters), then the reconstruction of that event can be weighted accordingly. This is expected to yield a noise free, better quality image<sup>17</sup> with improved spatial resolution.

This part of the method in PET is still under development, and a few experimental results<sup>18-21</sup> with new scintillators such as LSO and  $\text{LaBr}_3$  have been reported. In particular, LSO scintillators have been tried since they have a relatively high light yield (about  $30,000 \text{ photons}\cdot\text{MeV}^{-1}$ ), high effective  $Z$  ( $Z_{\text{eff}}=66$ ), high density ( $7.4 \text{ g}\cdot\text{cm}^{-3}$ ), short decay time (40 ns) and are used in commercially available PET scanners. With a single pair of detectors, a timing resolution of 220 ps has been measured with LSO and in a recent commercial LYSO TOF PET system (Philips), a 600 ps timing resolution has already been achieved.

A TOF PET system based on  $\text{LaBr}_3$  also is being developed<sup>21</sup> and promises an even better timing resolution and excellent energy resolution, but there may be some compromise in sensitivity because of lower stopping power of  $\text{LaBr}_3$  as compared to LSO and LYSO. The limitation in the ability to localize the

annihilation point is mainly due to the uncertainty on the measured time difference,  $\delta t$ , which is related to the time resolution  $\Delta t$  of the coincidence system. This uncertainty is implemented as a probability function for the localization of the detected annihilation and the FWHM of the probability function is the localization uncertainty of say point P as:  $\Delta p(\text{FWHM})=c \Delta t/2$ .<sup>18</sup>

The fundamental improvement brought about so far, by TOF is an increase in signal-to-noise ratio (SNR) that helps to resolve structures imbedded inside large objects. The approximate improvement over that obtained with non-TOF-PET is given by:

$$\text{SNR}_{\text{TOF}} \approx \sqrt{2D/c \Delta t} \times \text{SNR}_{\text{non-TOF}}$$

where  $D$  is the diameter of the object being imaged,  $c$  is the speed of light, and  $\Delta t$  is the timing resolution of the system.<sup>23</sup> With the advent of the newer scintillators with excellent time resolution, with good stopping power and without any compromise in efficiency, TOF-PET would offer a far better performance.

### A glimpse of the image reconstruction method

Since the early medical imaging applications,<sup>24</sup> the tomographic reconstruction procedure has grown into a highly evolved field.<sup>25</sup> We present here a focused outlay and the essential points for the reader, to understand the basic points of image reconstruction procedure for PET, in a simple way. In a PET scanner system, information about coincidences between detector pairs are registered and collected along a line of response (LOR). Unscattered photon pairs recorded for a specific LOR arise from annihilation events located within a thin volume centered around the LOR. This volume typically has the shape of an elongated thin pipe and is referred to as a tube of response as shown in Fig. 9. Since the detectors have a finite size, a number of LOR are contained in practice, within a tube of finite dimension. In the absence of the physical effects such as: attenuation, scattered and accidental coincidences, detector efficiency variations or count rate dependent effects, the total number of coincidence events detected will be proportional to the total amount of tracer contained in the tube of response.



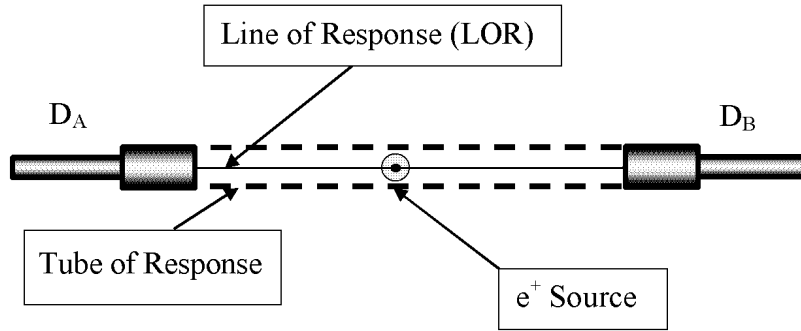


Fig. 9. Schematic representation of the tube of response that includes the radiotracer distribution

To each pair of detectors  $D_A D_B$ , is associated an LOR and a sensitivity function:

$$\zeta_{DADB}(r = (x,y,z))$$

such that the number of coincident events detected is a Poisson variable within a mean value, in the field of view (FOV):

$$\langle \phi_{DADB} \rangle = \tau \int_{FOV} dr f(r) \zeta_{DADB}(r)$$

where  $\tau$  is the acquisition time and  $f(r)$  denotes the tracer concentration, that is stationary and non existent beyond the (FOV). The reconstruction problem then consists of recovering  $f(r)$  from the acquired data  $\phi_{DADB}$  from a large number of detector pairs in modern scanners. It also assumes that the data have been pre-corrected for randoms, scatter and attenuation and that the sensitivity function is only considered along the tube of response as shown in Fig. 9. With these impositions, the data are modeled as line integrals of tracer distribution within (FOV).

The number of positron-electron annihilations associated with each LOR is proportional to the sum of the tracer concentration within that LOR. This sum approximates a line integral of the tracer concentration along the LOR. The closeness of the geometry of the tube to a true line integral is evidently related to the finite size of the detectors, i.e., smaller radius of the LOR gives better approximation of a true line integral.

### 2D image reconstruction (standard parameterization of 2D PET data into sinograms)

There are several ways<sup>16,26</sup> to reconstruct a PET image,<sup>16,25</sup> for example: consider a transaxial section  $z=z_0$  is measured using a ring of detectors, to recover information consisting of projections,  $p(s,\theta)$ . The image reconstruction algorithms try to transform the projections to an image of the tracer distribution,  $f(x,y)$ ,

(Fig. 10). From a mathematical point of view, the projection  $p(s,\theta)$  approximates a line integral through the tracer distribution  $f(x,y)$  at a particular angle  $\theta$  (this angular variable specifies the orientation of LOR) and at a particular radial distance  $s$ , from the origin. The set of line integrals of the tracer distribution are described as:

$$p(s,\theta) = \int_{-\infty}^{\infty} dt f(x = s \cos \theta - t \sin \theta + t \cos \theta)$$

where  $t$ , the integration variable, is the coordinate along the line.

The function  $p(s,\theta)$  is referred to as sinogram. The geometrical arrangement of discrete detectors determines a set of samples  $(s,\theta)$  in sinogram space. In this text we have only touched upon the basics of the data collection system, that leads to image reconstruction. In short, PET reconstruction algorithms can be basically divided into analytical methods or stochastic/iterative methods. Analytical methods rely on Fourier transforms to derive the point spread function from the source distribution, while the iterative methods recognize the statistical nature of the data and model them into algorithm. The detailed discussion of this section is, however, beyond the scope of this article.

When using TOF PET, one has to store the time-of-flight (TOF) information of each coincidence and the sinogram as mentioned above, is no longer adequate. In TOF PET one can also approximately note where on that line the annihilation has occurred, following the principles as outlined in the earlier section.<sup>27</sup> For the detailed mathematical model<sup>28</sup> of TOF PET and image improvements in PET, evaluation on maximum-likelihood estimates as a function of TOF uncertainty, one could refer to Reference 29.

### Application of radiotracers and kinetic modeling

The subject area basically deals with bio-radiochemistry with positron emitting tracers. Over the past decades more than a thousand molecules were

labeled with positron emitters targeting various molecular processes in the human body.<sup>30</sup> The availability of positron emitting isotopes for some of the most prevalent elements in organic molecules (such as C, N, O and F) allows one to label virtually any molecule of interest. Further, each tracer must be targeted to measure a physiological parameter of interest such as blood flow, metabolism, receptor content, etc., in one or more organs or regions. After injection of tracer into a patient, high quality three dimensional image is produced, by state-of-the-art PET instrumentation which eventually suggests quantitative measurements of regional radioactivity concentration.

To this aspect, the tracer kinetic modeling<sup>1</sup> plays a vital role: if an appropriate tracer is selected and suitable imaging conditions are used, the activity values measured in a region of interest (ROI), in the image should be most heavily influenced by the physiological characteristic of interest, be it blood flow, receptor concentration, etc. Thus, a suitable tracer kinetic model can account for all the biological factors that contribute to the tissue radioactivity signal. The assay of the radiotracer concentration in a particular region of tissue, after a certain time period have elapsed, since its injection is dependent mainly on the local physiology, e.g., the blood flow/metabolism in that region and time course of tracer concentration in the blood or plasma, which in turn defines its availability to the target organ. Quite often, mathematical relationship is used to describe or to relate the controlling physiological factors, the concentration of the tracers in the tissue and answer the question related to clinical investigation. It

is, however, very important to have a proper choice of the radiotracer and the pharmaceutical compound to which it may be bound, for the specifically aimed physiological parameters or else other extraneous factors may affect its distribution and kinetics in the body. Recently tumor imaging using <sup>68</sup>Ga labeled DOTA-conjugated peptides became one of the most exciting approaches to diagnose neuroendocrine and other tumors and metastases because: (1) octreotide derivatives have high affinity and selectivity to somatostatin receptor expressing tumor cells, (2) syntheses of DOTA-conjugated targeting vectors are straight forward due to kit type labeling and their PET/CT scanners perfectly correlate morphological and functional parameters.<sup>31-34</sup> However, the most common attempts are with <sup>18</sup>F, since it possesses a convenient half-life for the entire pre-scheduled procedures for the specimens and uptake is increasingly found in the tumour cells through a labeled glucose FDG (2-deoxy 2-fluoro-D glucose), which is used to examine physiological processes like glucose metabolism (for detailed studies one may consult References 16 and 35).

#### Some critical points of the present state of the art of PET

It has been observed that there are wide variations in the PET systems, starting most fundamentally from the different varieties of the detectors chosen<sup>36-38</sup> to the various types of configurations used, restricted field view (<http://depts.washington.edu/nucmed/IRL/publications.html>) to large, open field designs.

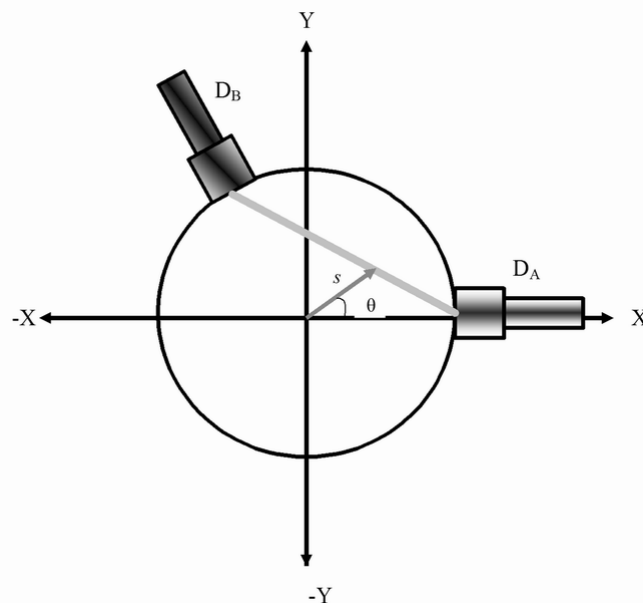


Fig. 10. Schematic representation for a ring scanner, a tube of response between two detectors  $D_A$  and  $D_B$  is shown that connects the front face of the two detectors. The sinogram variables  $s$ ,  $\theta$  define the tracer distribution  $f(x,y)$  in the LOR

There are important points also as regards the choice of suitable radiotracers that would exactly bind at the molecular level. For example, for a receptor binding radiotracer, regional radioactivity concentration data are affected by regional blood flow, plasma protein binding, capillary permeability, nonspecific tissue binding and so many other factors within the body. Thus for a well designed tracer, the net effect of these extraneous factors would be minor. Apart these, there are other factors that need to be mentioned: (a) positrons emitted from a radiolabeled compound bound to a particular molecular site (in the tissue) may diffuse after losing its kinetic energy, (b) a fraction of emitted positrons may also form Positronium (Ps) state. The mean diffusion length of positron or positronium species is expressed as:  $l = \sqrt{\tau D}$ , where  $\tau$  and  $D$  are the life-time and diffusion coefficients of the species, respectively.  $D$  is evidently dependent of the tissue media and could be of the order  $\sim 10^{-3} \text{ cm}^2/\text{s}$  for positrons or even more. This would mean that due to Brownian motion, these thermal positrons would be distributed (isotropically) over a microscopic area (mean diffusion length  $\sim 1000 \text{ \AA}$  or more) and would contribute to the uncertainty in localization of the tracer atom and spatial dimension of the image (Fig. 11). Since the annihilation sites and not the site of radioactive atoms are imaged by PET, some blurring will be introduced. The extent of blurring (spreading of the image) is of important concern because the imaging technology involved here is at molecular level, and at nanometer scale, specially for drug designing and testing in small animal PET system.

However, for positronium species,  $D$  is much smaller, because of its neutral charge, high polarizability and localization. But these species would follow a different chemical and kinetic behavior at the binding site, because Ps atom chemistry is quite different from that of the tracer atom (positron emitter) used for

targeting (at the molecular binding site). In addition, the annihilation characteristics of Ps states (ortho and para states of positronium atom and its association with a molecule) are also quite different from positrons. The kinematics of annihilation rate constant would vary (not so straight forward as in the case of direct positron annihilation). It is well known that for para-Ps the decay rate constant is  $7.98 \cdot 10^9 \text{ s}^{-1}$ , while for ortho-Ps it is much slower,  $7.04 \cdot 10^6 \text{ s}^{-1}$  (in vacuum) but it has a pick off process in a molecular media.<sup>39</sup> This annihilation rate in a given tissue (medium) would have an impact on the actual signal processing, depending up on the formation intensity of positronium species in the medium and their reaction with the biological molecules. These minute details have not yet been taken into account so far, as too many features would complicate the issue of the image formation algorithm.

The subject of positronium chemistry itself constitutes important micro environmental studies of the exotic species namely Ps quasi stationary state, which actually would hint the malfunctioning or any change from the normal condition at the site of binding. Ps species is a good chemical probe<sup>39</sup> and mimicking the situation with proper in-vitro experiments would suggest important information (such as molecular level phase transition effecting the physiological function at a given site) which may not have been discovered due to the blurring of the PET images. Collaborative investigations in this direction with positronium chemistry may frame out in near future, as we see that these topics and various other prospective discussion has been included in the international workshop: Positron and Positronium Chemistry-8 in 2005, Coimbra, Portugal.<sup>40</sup> Also one could refer to the attempt made by Y. C. JEAN in investigating skin carcinoma by slow positron beam technique.<sup>41</sup>

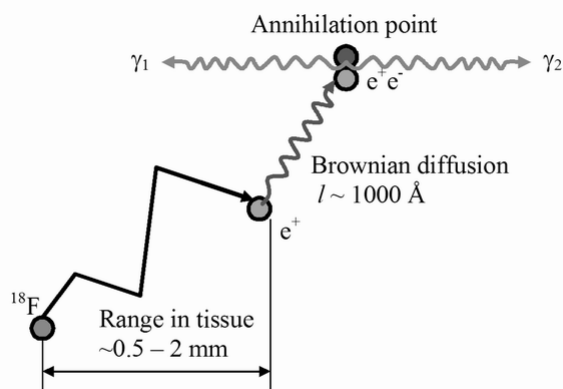


Fig. 11. Simple illustrative figure for positron distribution in medium, considering FDG uptake (a modified version of Fig. 1)

There are, of course, many other factors which determine the measuring performance of PET systems. The most important of them is spatial resolution (as has been mentioned above). This refers to the minimum limit of the system's spatial representation of an object due to the measurement process. There is often an undue broadening or blurring effect. The common method to measure this in emission tomography is to image a point source of radioactivity (with a spread function). The resolution of the profile is measured as the full-width at half-maximum (FWHM) of the Gaussian which is given by the expression  $\text{FWHM} = 2.35 \sigma$  (standard deviation) for this profile. This itself depends upon many factors such as: emitted positron range, diffusion of the same, non-colinearity of the electron-positron annihilation photons (resulting in angular deviation, Doppler shift in energy), the detectors employed, their stopping power, size and shape, distance between them, matrix resolution, and the reconstruction parameters (matrix size, windowing of the reconstruction filter, etc.). The other serious inherent limitation of blurring effect lies with the range of the positrons, especially from nuclei like  $^{68}\text{Ga}$ , and further spread due to diffusion of positron in the medium. A mathematical recovery of full spatial resolution using Fourier transform analysis was tried<sup>42</sup> but seemed impractical due to the increase in statistical noise level. On the other hand, a Monte Carlo simulation study on positron flight on human tissues and its influence on spatial resolution shows large variation depending on the nature of the tissue (density of the tissue material) and the energy of the positrons emitted from different radionuclides.<sup>21</sup> However, in clinical situations, the spatial resolution depends more on the number of counts that have been collected. There are also other correction factors like scatter fraction, random events, dead-time loss and the counting efficiencies of the detectors, all of which contribute to the effective sensitivity of the positron emission tomography. This is still an important issue and would require a large increase of the collected counts under study. Such improvements are some what easier to realize in a small animal scanner system than in a human scanner, because the animal can almost be surrounded by detectors, without requiring an unreasonable amount of detector material, ensuring all the photon pairs intersect the detector system. When detectors that measure depth of interaction are used,<sup>43</sup> or thicker detectors are used in small animal PET, increase in sensitivity more than 5–10 fold is possible.<sup>23</sup>

The sensitivity of positron emission tomograph has traditionally been measured using a distributed source of a relatively long-lived tracer, such as  $^{18}\text{F}$ , in water. The value was quoted in units of counts per second per microcurie, per milliliter ( $\text{counts}\cdot\text{s}^{-1}\cdot\mu\text{Ci}^{-1}\cdot\text{mL}^{-1}$ ) in non SI units, without correction for attenuation or scattered radiation. However, a much improved version has been

employed recently,<sup>44</sup> which uses a known amount of  $^{18}\text{F}$  in a small source holder made from aluminum of sufficient thickness to stop all the positrons. The annihilation events are then counted for a defined period in the camera. A calibration of the aluminum thickness, and attenuation produced is used to produce an attenuation curve, the extrapolated 'y' intercept of this curve gives the 'sensitivity in air' ( $\text{counts}\cdot\text{s}^{-1}\cdot\text{MBq}^{-1}$ ) for the camera.

There are formal governing bodies like NEMA (Performance measurements of positron emission tomograph, Washington: National Electrical Manufacturers Association; 2001.Report No.NU2-2001) in USA who assess the whole body PET test procedures. Europe has IEC (International Electrochemical Commission) as set standard to measure their performance. However, the difficulty exists for extrapolating the performance in standard test to the clinical situations (that is sometimes unrealistic).

Improvement and updating of the procedure regularly continues. At the present time, a combined scan of PET/CT has shown to yield much superior image quality by doing the attenuation scan from the CT information. To acquire the PET/CT image, a patient passes through the CT portion of the scanner first and then through the PET scanner where the metabolic information is acquired. When the patient has passed through both portions, a merged or fused image can be created. Perhaps with due course of time, positronium fraction in the region of interest would also be accounted, making proper justice towards its intensity parameter (accountability for the different annihilation rate, and hence, subtle contrast/brightness of the structure), to be more accurate in interpretation in view of medical diagnoses. Prediction of the future is difficult, but it is apparent that ample scope exists for new development and innovation, that will be driven by molecular medicine, with specific molecular diagnostic tools and the ability to quantitatively monitor therapeutic entities that include small molecules, peptides, antibodies, nanoparticles, DNA/RNA and cells. Currently, PET is emerging as modern tool in molecular imaging technology, in true sense it would offer many opportunities for advancement and improvements depending on its applications.

### **Radiation dosimetry and protection in PET**

Despite the high energy of the annihilation photons, the short half-lives of clinical PET isotopes limit the internal radiation dose to patients. The radiation dose to patients is often comparable to that from other diagnostic nuclear medicine procedures which employ single photon emission. The absorbed dose is limited by short physical half-life and the maximum amount of activity that can be administered to the patient.

The maximum amount of [ $^{18}\text{F}$ ]-FDG that can be administered to a “standard” 70 kg adult person for whole body oncology study is 200 MBq for detection with a NaI coincidence gamma camera, less than 500 MBq for BGO camera in 3D mode, and may be higher for fast LSO detectors.

According to the Medical Internal Radiation Dose method,<sup>45</sup> the dose to a target organ from radioactivity in a source organ is given by:

$$D_{st} = \tilde{A}_s \cdot S_{st}$$

where  $\tilde{A}_s$  is the cumulated activity in the source organ and  $S_{st}$  is the absorbed dose in the target organ per unit cumulated activity in the source organ.  $\tilde{A}_s$  represents the total number of disintegration of the radionuclide occurring in the source organ and can be determined from the relation:

$$\tilde{A}_s = 1.44 F_s A_0 t_{1/2}(\text{eff})$$

where  $A_0$  is the administered activity,  $F_s$  is the fraction of  $A_0$  representing initial rapid uptake,  $t_{1/2}(\text{eff})$  is the effective half-life of the radioisotope due to biological clearance and radioactive decay and is given by:

$$\frac{1}{t_{1/2}(\text{eff})} = \frac{1}{t_{1/2}(\text{biol})} + \frac{1}{t_{1/2}(\text{rad})}$$

$S_{st}$  is determined from the physical properties of the radionuclides and tabulated values for pairs of source and target organs are available for many radionuclides.<sup>46</sup> In the case of administered [ $^{18}\text{F}$ ]-FDG estimated absorbed dose to some of the maximally exposed organs are 0.16 mGy·MBq<sup>-1</sup> for bladder, 0.062 mGy·MBq<sup>-1</sup> for the heart, 0.028 mGy·MBq<sup>-1</sup> for the brain, and 0.021 mGy·MBq<sup>-1</sup> for the uterus.<sup>47</sup> Presently, the literature survey shows that more data collection for radiation dose estimates for selected PET radio-pharmaceuticals comprising mainly of  $^{11}\text{C}$ ,  $^{18}\text{F}$  and to certain extent of  $^{15}\text{O}$  is needed. As well as the application of other radionuclides such as  $^{68}\text{Ga}$  needs to be carried out for future applications.

## Conclusions

It has been realized, PET by itself is a vast research area, under which each small subdomain needs special attention by various kinds of specialists since it deals with different kinds of subjects and hence, is truly multidisciplinary in nature. It is also amazing to note the vast development taking place in every sector (from basic science of detector development to sensing of the radiation, instrumentation, data handling for the tomography and also the radiological aspects) of which only a few important ones have been mentioned here. For the success of PET image reconstruction, and hence, the medical diagnoses, innovation in each area is highly

interlinked and very neatly interwoven, as if driven by some strong miraculous team spirit, for the responsibility lies with each small aspect of new development. In future years to come, it is expected to open up new prospective for all kinds of research groups depending up on the need of medical and life science research.

\*

We thankfully acknowledge the encouragement received in various forms from the Director of Saha Institute of Nuclear Physics in order to continue our work in the direction of PET.

## References

1. P. E. VALK, D. L. BAILEY, D. W. TOWNSEND, M. N. MAISEY, Positron Emission Tomography: Basic Science and Clinical Practice, Springer-Verlag, Ltd., London, 2003, p. 147.
2. S. KERSTIN, B. WOLFGANG, P. MOHR, A. ZILGES, Am. J. Phys., 70 (2002) 929.
3. M. A. MANDELKERR, Annu. Rev. Nucl. Sci., 45 (1995) 205.
4. S. J. OFFORD., D. F. WONG., S. NYBERG, J. Clin. Pharmacol. Suppl., (1999) 17s.
5. W. BRANDT, R. PAULIN, Phys. Rev., B15 (1977) 2511.
6. D. M. SCHRADER, Y. C. JEAN, Positron and Positronium Chemistry, Elsevier, 1988.
7. O. E. MOGENSEN, J. Chem. Phys., 60 (1974) 998.
8. V. M. BYAKOV, V. I. GOLDANSKII, V. P. SHANTAROVICH, Dokl. Akad. Nauk SSSR, 219 (1974) 633 [Dokl. Phys. Chem., 219 (1974) 1090].
9. R. FEYNMAN, Quantum Electrodynamics, Benjamin/Cummings Publ. Inc., Reading, Mass, 1982.
10. G. F. KNOLL, Radiation Detection and Measurement, 2nd ed., John Wiley and Sons, New York, 1988.
11. C. PEPPIN MICHELLE et al., IEEE Trans. Nucl. Sci., 51 (2004) 789.
12. S. I. ZIEGLER, B. J. PICHLER, G. BOENING, M. RAFECAS, W. PIMPL, E. LORENZ et al., Eur. J. Nucl. Med., 28 (2001) 136.
13. S. R. CHERRY, Y. SHAO, R. W. SILVERMAN, A. CHATZIIAONNOU, K. MEADORS, S. SIEGEL et al., IEEE Trans. Nucl. Sci., 44 (1997) 1161.
14. M. BERGSTROM, L. ERICKSSON, C. BOHM, G. BLOMQUIST, J. E. LITTON, J. Comput. Ass. Tomogr., 7 (1983) 42.
15. C. CARRIER MARTEL, C. SCHMITT, R. LECOMTE, IEEE Trans. Nucl. Sci., NS-35 (1988) 685.
16. D. L. BAILEY, D. W. TOWNSEND, P. E. VALK, M. N. MAISEY, Positron Emission Tomography: Basic Sciences, Springer-Verlag, London, 2005, Chapter-3.
17. WAI-HOI WONG, N. A. MULLANI, G. WARDWORTH, R. K. HARTZ, IEEE Trans. Nucl. Sci., NS-31 (1984) 381.
18. C. MAURIZIO et al., Phys. Med. Biol., 50 (2005) 4507.
19. T. YAMAYA, T. OBI, M. YAMAGUCHI, N. OHYAMA, Phys. Med. Biol., 45 (2000) 3125.
20. M. DEFRISE, M. CASEY, M. CHRISTIAN, C. MAURIZIO, Phys. Med. Biol., 50 (2005) 749.
21. S.-C. ALEJANDRO, A. PEDRO, A. S. LARSSON, Eur. J. Med. Mol. Imag., 31 (2004) 44.
22. A. KUHN, S. SURTI, J. S. KARP, G. MUEHLEHNER, F. M. NEWCOMER, R. VAN BERG, IEEE Trans. Nucl. Sci., 53 (2006) 1090.
23. S. R. CHERRY, J. Nucl. Med., 47 (2006) 1735.
24. A. ALESSIO, P. KINAHAN, T. LEWELLEN, Improved Quantization for PET/CT Image Reconstruction with System Modeling and Anatomical Priors, SPIE Med. Imaging, San Diego, 2005.

25. F. NATTERER, F. WUEBBELING, *Mathematical Methods in Image Reconstruction*, SIAM Monographs on Mathematical Modeling and Computation, 2001.
26. D. W. TOWNSEND, R. A. ISOADI, B. BENDRIEM, *Volume Imaging Tomographs: The Theory and Practice of 3D PET*, B. BENDRIEM, D. W. TOWNSEND (Eds), Dordrecht, Kluwer Academic, 1998, p. 111.
27. W. W. MOSES, *IEEE Trans. Nucl. Sci.*, 50 (2003) 1325.
28. D. L. SNYDER, T. J. LEWIS Jr., M. M. TER-POGOSSIAN, *IEEE Trans. Nucl. Sci.*, (1981) NS-28, (3).
29. D. G. POLITE, *IEEE Trans. Nucl. Sci.*, 37 (1990) 737.
30. A. J. ABRUNHOSA, *Biochemistry with positron emitting tracers*. Abstract, in: 8th Intern. Workshop on Positron and Positronium Chemistry, Positrons in Medicine Symp. 4–9 September 2005; Symposium: Positrons in Nuclear Medicine. *Radiat. Phys. Chem.*, 76 (2007) 337.
31. F. RÖSCH, *Indo German Workshop on Recent Trends in Development of PET Radiopharmaceuticals*, November 15–17, 2005.
32. M. HOFMANN, H. R. MÄCKE, A. R. BÖRNER, E. WECKESSER, P. SCHÖFFSKI, M. L. OEI, J. SCHUMACHER, M. HENZE, A. HEPPELER, G. J. MEYER, W. H. KNAPP, *Eur. J. Nucl. Med.*, 28 (2001) 1751.
33. G-J. MEYER, H. R. MÄCKE, J. SCHUHMACHER, W. H. KNAPP, M. HOFMANN, *Eur. J. Nucl. Med.*, 31 (2004) 1097.
34. R. H. MAECKE, M. HOFMANN, U. HABERKORN, *J. Nucl. Med.*, 46 (2005) 172S.
35. M. R. KILBOURN, *Fluorine-18 Labeling of Radiopharmaceuticals*, Nuclear Science Series NAS-NS-3203, National Academy Press, Washington DC, 1990.
36. M. E. PHELPS, E. J. HOFMANN, S. C. HUANG, D. E. KUHL, *J. Nucl. Med.*, 19 (1978) 635.
37. M. E. CASEY, R. NUTT, *IEEE, Trans. Nucl. Sci.*, NS-33 (1986) 460.
38. N. INADAMA, H. MURAYAMA, T. OMURA et al., *IEEE Trans. Nucl. Sci.*, 49 (2002) 629.
39. H. J. ACHE (Ed.), *Positronium and Muonium Chemistry*, American Chemical Society, Washington D.C., 1979.
40. J. J. PEDROSO DE LIMA, *Radiat. Phys Chem.*, 76 (2007) 360. Abstracts: Positrons in Nuclear Medicine: 8th International Workshop on Positron and Positronium Chemistry 4–9 Sept 2005, Universidade de Coimbra, Portugal.
41. B. GANGULY et al., *National Seminar: Positron Annihilation*, held on 9–10 February, 2007 at Saha Institute of Nuclear Physics, Kolkata, India, [adsabs.harvard.edu/abs/2007cond.arxiv.org/pdf/cond-mat/0703056](http://adsabs.harvard.edu/abs/2007cond.arxiv.org/pdf/cond-mat/0703056)
42. S. F. HABER, S. E. DERENZO, D. UBER, *IEEE Trans Nucl. Sci.*, NS-37 (1990) 1293.
43. J. SEIDEL, J. VAQUER, S. SEIGEL, W. R. GANDLER, M. V. GREEN, *IEEE Trans. Nucl. Sci.*, 46 (1999) 485.
44. D. L. BAILEY, T. A. JONES, *Eur. J. Nucl. Med.*, 24 (1997) 660.
45. R. LOEVINGER, T. F. BUDINGER, E. WATSON, *MIRD Primer for Absorbed Dose Calculation*, Society of Nuclear Medicine, New York, 1988.
46. W. S. SNYDER, M. R. FORD, G. G. WARNER, S. B. WATSON, *Absorbed dose per unit cumulated activity for selected nuclides and organs*, MIRD Pamphlet No. 11, Society of Nuclear Medicine, New York, 1975.
47. ICRP 1998, *Radiation Dose to Patients from Radiopharmaceuticals*, Addendum to ICRP-53, Publication 80, Pergamon Press, Oxford.